Mailed to J.P.C.S. 3/16/88

(1)

^{31}P Solid State NMR Studies of ZrP, Mg_3P_2, MgP_4, and $CdPS_3$

1988

R. A. Nissan and T. A. Vanderah*

Chemistry Division, Research Department

Naval Weapons Center, China Lake, CA 93555

AD-A199 981

ABSTRACT: The ^{31}P solid state NMR spectra of ZrP, Mg_3P_2, MgP_4, and $CdPS_3$ are reported. Static and magic angle spinning (MAS) spectra were obtained for each compound. In all cases, chemical shift anisotropy and the effects of dipolar broadening were sufficiently reduced by the MAS method to reveal the isotropic chemical shifts for each crystallographically distinct phosphorus. The observed resonances were assigned to the different types of phosphorus by considering the structural details of each compound. In ZrP the two chemical shifts of +128.4 and +187.5 ppm (relative to 85% H_3PO_4) were assigned to P occupying the Wyckoff 2d and 2a sites, respectively. In Mg_3P_2, two resonances from the 24d and 8a site P atoms were observed at -262.3 and -239.6 ppm, respectively. In MgP_4 two types of phosphorus, one type coordinated to two Mg and two P and the other to three P and one Mg, gave chemical shifts of -109.2 and -6.1 ppm, respectively. From $CdPS_3$ only one resonance at +104.9 ppm is observed as all P atoms are crystallographically equivalent. Zirconium Phosphide, Magnesium Phosphide, Cadmium thiophosphide, (trigonal)

KEY WORDS: P-31 MAS NMR; Solid State NMR; ZrP; Mg_3P_2; MgP_4; $CdPS_3$

88 8 31 08

INTRODUCTION

The development of magic-angle-spinning nuclear magnetic resonance (MAS NMR) spectroscopy has greatly facilitated multinuclear studies of solid state samples. Review texts [1,2] and articles [3,4] have appeared which discuss the methods in detail.

Liquid state NMR spectra are characterized by sharp resonances with clearly discernible isotropic chemical shifts: on the NMR time scale, molecular tumbling is fast and produces "motional narrowing" - an averaging of various line-broadening effects arising from interactions of the nuclei with other nuclei and with electric field gradients due to anisotropic chemical environments. In contrast, the absence of Brownian motion in solids as well as the extended nature of the chemical bonding make them predisposed to severe line-broadening effects, and line-narrowing techniques such as MAS must be used to obtain well defined NMR spectra.

Under MAS conditions, the equations describing most of the line-broadening interactions in solids depend on the term $3\cos^2\theta-1$, where θ is the angle between the applied magnetic field and the axis about which the sample is spinning. This term vanishes at $\theta = 54.7°$ (the magic angle). Therefore, if the sample is rotated about an axis inclined 54.7° to the applied magnetic field, most broadening effects are reduced to zero since all nuclei have been effectively placed on this axis by the process of rapid spinning about it. MAS also averages the orientation-dependent contributions to the chemical shielding and reveals the solution-like isotropic chemical shift. The chemical shift anisotropy, which can be observed in the shapes of the broad resonances obtained under non-spinning conditions, is a measure of the asymmetry of the electric field surrounding the nucleus under investigation. If the sample

spinning frequency is less than the line width of the chemical shift anisotropy, part of the resonance signal is displaced into spinning sidebands which flank the isotropic signal; the chemical shift values of the sidebands differ from that of the isotropic signal by multiples of the spinning frequency.

Application of MAS NMR to the characterization of solids is particularly important in cases where X-ray diffraction is of limited utility; e.g., the aluminosilicates, such as zeolites, which are often poorly crystalline in addition to requiring differentiation between Al and Si, which differ by only one atomic number. Numerous ^{29}Si and ^{27}Al MAS NMR studies on this class of compounds [4-6] have demonstrated the usefulness of the method in elucidating local structural environments.

The ^{31}P nucleus (S = 1/2) has a natural abundance of 100% and is easily probed by NMR. Extensive solution state ^{31}P NMR studies have been carried out on biological and organic systems [7] and on organometallic phosphine derivatives [8-10]. Reports have recently appeared on solid state studies of inorganic phosphates [4,11], pyrophosphates [12], and phosphate glasses [4,13]. Non-molecular inorganic phosphorus-containing compounds have been the least studied, although reports have appeared on sphalerite-type InP and GaP [14], chalcopyrite-type $ZnSnP_2$ [15], and the chalcopyrite-type series $ZnSiP_2$, $ZnGeP_2$, and $ZnSnP_2$ [16].

At the present time, theoretical calculations of chemical shift values in ^{31}P NMR spectra are not possible [4,7]. ^{31}P resonance positions are extremely sensitive to a variety of complex and interrelated factors such as the variation of the hybridization of phosphorus, which may involve s, p, and d orbital contributions; inductive factors due to chemical bond type; local coordination geometry; and formal

A-1

oxidation state. Much of the recent work on MAS NMR of solids has therefore involved structurally and chemically well characterized compounds in order to establish qualitative relationships and an interpretative data base which might be extended to less well characterized samples. We report here the ^{31}P solid state NMR spectra and detailed structural discussions of the non-molecular inorganic solids ZrP, Mg_3P_2, MgP_4, and $CdPS_3$.

EXPERIMENTAL METHODS

Hexagonal ZrP was obtained commercially (CERAC, 99.5%). Attempts to obtain the cubic form from this commercial product by quenching in liquid nitrogen from 1025°C were not successful. Loss of phosphorus is necessary to stabilize cubic ZrP [17,18]; therefore, $ZrP_{0.92}$ was prepared from stoichiometric amounts of the elements which were ground together, sealed in an evacuated silica ampule, and heated at 800 to 900°C for 2 d. After cooling over 24 h to room temperature, only the hexagonal phase was detectable by X-ray diffraction; however, after reheating at 1100°C for 12 h and quenching in liquid nitrogen, the cubic form was clearly present in the X-ray diffraction pattern, although 80 to 90% of the sample retained the hexagonal structure. Mg_3P_2 was obtained commercially (Pfaltz & Bauer). MgP_4 was prepared as a byproduct in the attempted syntheses of $MgGeP_2$ [19]. $CdPS_3$ crystals were grown from the elements [20].

Samples were identified by X-ray diffraction (Cu Kα radiation) using a Scintag PAD V powder diffractometer, the Gandolfi method for crystals, and/or the Debye-Scherrer method.

^{31}P NMR spectra were obtained with an NT-200 WB spectrometer equipped with a magic angle spinning probe. The probe was tuned to 81 MHz and an external sample of 85% phosphoric acid was used as the reference standard. Samples were ground and packed into a 7 mm diameter rotor and spun at 3 to 5 kHz. Non-spinning spectra were also recorded. When sample quantities were limited, approximately 5 mg of the compound was mixed with KBr prior to loading. Spectra were acquired by a one-pulse method using a 30° pulse and a 10 s recycle time. Spectra were usually obtained in an hour or less, but experiments involving small amounts of material or broad resonances required overnight data acquisitions.

RESULTS AND DISCUSSION

ZrP. Hexagonal ZrP adopts a structure with space group $P6_3/mmc$ (a =3.684, c = 12.554 Å) [18,21]. Zr atoms occupy the Wyckoff 4f positions while the P atoms are equally distributed in the 2a and 2d sites. The structure can be described using close-packing terminology: phosphorus atoms form hexagonally close-packed layers in the sequence, along the c-axis, ABCB. Zirconium atoms occupy all octahedral sites between the P layers. The structure can therefore be thought of as interpenetrating slabs of NaCl-like (ABC) and NiAs-like (BCB) sandwiches. The coordination of phosphorus by zirconium alternates along the c-axis from octahedral (2a site) in the NaCl-like slabs to trigonal prismatic (2d site) in the NiAs-like slabs. The two different coordination geometries of phosphorus are depicted in Figure 1. The two types of phosphorus are clearly distinguished in the ^{31}P NMR spectra shown in Figure 2. The static spectrum shows partial resolution of the two axially symmetric resonances which are of comparable intensity, as expected from the equal distribution of phosphorus in the two crystallographic sites. Spinning at the magic angle resolves

the resonances, revealing the isotropic signals A and B at +128.4 and +187.5 ppm, respectively. The sample spinning frequency, however, is considerably less than the chemical shift anisotropy which is reflected in the intensities of the spinning sidebands a_1 to a_4 and b_1 to b_4. In order to assign the resonances to the different types of phosphorus, the ^{31}P MAS NMR spectrum of the cubic form of ZrP, which has the NaCl structure and therefore only octahedrally coordinated phosphorus, was sought. The ^{31}P NMR spectra of $ZrP_{0.92}$, which exhibited 10 to 20% conversion to the cubic form and therefore enrichment in octahedral phosphorus, are shown in Figure 3. Enhancement of the downfield B signal at +187.5 ppm is seen in the MAS spectrum and this resonance is assigned to octahedral phosphorus. The downfield position of the signal may be related to a greater number of 90° bonding interactions, which are associated with large downfield shifts of ^{31}P NMR signals in organometallic phosphine-derived systems.[8-10] In octahedral coordination the Zr-P-Zr bond angles are either 90° (twelve) or 180° (three). In the trigonal prismatic site the Zr-P-Zr bond angles, calculated from the reported interatomic distances [18], are 91.6° (six), 137.2° (six), and 72.8° (three). In both coordination sites the Zr-P bond lengths are 2.643 Å [18].

Mg_3P_2. Mg_3P_2 adopts the cubic anti-bixbyite structure [22,23]. Numerous sesquioxides, including many of the rare earth elements, exhibit the cubic bixbyite structure. The anti-bixbyite structure of Mg_3P_2 is derived from the cubic bixbyite structure of the metal sesquioxides by switching the metal and nonmetal positions: magnesium occupies the oxygen position and phosphorus the metal position. There are 16 formula weights per unit cell (Ia3, a =12.01 Å); the 48 Mg atoms are located in the Wyckoff 48e site, and the 32 P atoms fill the 8a and 24d sites. Therefore, two crystallographically different types of phosphorus are present in a ratio of 1:3. Both phosphorus positions are 6-coordinate by Mg, as illustrated in Figure 4 [24]. The

overall structure is related to that of fluorite, CaF_2, in which the coordination of Ca is cubic. The bixbyite structure is obtained by removing one-fourth of the fluoride ions and allowing all the atom positions to shift slightly. At the former Ca sites, or P sites in Mg_3P_2, there are now 6-coordinate positions of two types. Each is derived from a cubic arrangement by removing two of eight vertices. For one-fourth of the positions (8a site) these two are at the ends of a body diagonal, and for the remainder (24d site) at the ends of a face-diagonal, as shown in Figure 4. The Mg atoms are 4-coordinate by P in approximately regular tetrahedra. The ^{31}P NMR spectra of Mg_3P_2 are given in Figure 5. The chemical shift anisotropy is evident in the asymmetric non-spinning spectrum, but is greatly reduced in the MAS spectrum which reveals two isotropic chemical shifts A and B at -262.3 and -239.6 ppm, respectively. The relative intensities are in agreement with the 1:3 crystallographic distribution of phosphorus. The upfield and more intense signal A is assigned to three-fourths of the P atoms which occupy the 24d site; the less intense and downfield signal B arises from those occupying the 8a site. The bond lengths and angles about P were calculated from the published crystallographic data [22]. For the 8a site the P-Mg bond lengths are equivalent at 2.649 Å; the Mg-P-Mg bond angles are 74.4° (six), 105.6° (six), and 180° (three). For the 24d site the P-Mg bond lengths are 2 @ 2.555, 2 @ 2.577, and 2 @ 2.604 Å; the bond angles are 76.6° (six), 94.1° (one), 102.7° (two), 110.6° (two), 112.8° (one), 130.4° (one), and 169.5° (two). The bond lengths in the 24d site are significantly shorter than those in the 8a site. This may account for increased shielding of phosphorus because of its closer approach to the electropositive metals; however, the differences in bond angles indicate differences in the hybridization of phosphorus which could be equally important. Two ^{31}P solid state NMR studies of Mg_3P_2 have previously been reported [25,26]. The spectrum obtained in the present study is consistent with the results of Kessemeier and

Norberg [25], who also reported two resonances separated by 24 ppm; however, Gibby et al. [26] reported an additional broad resonance 225 ppm downfield.

MgP_4. This compound is isotypic to CdP_4 and crystallizes in the monoclinic space group $P2_1/c$ (a = 5.144, b = 5.085, c = 7.526 Å, β = 98.66°, Z = 2 formula weights per unit cell) [27]. The two Mg atoms per unit cell occupy the Wyckoff 2a sites while the eight P atoms are equally divided into two sets of general 4e positions. Each phosphorus is pseudo-tetrahedral, one type (P_1) is bonded to two Mg and two P at 2.608, 2.635, 2.184, and 2.185 Å, respectively, with bond angles 114.3°, 101.6°, 120.1°, 105.7°, 108.9°, and 105.2° [27]. The other type of phosphorus (P_2) is bonded to one Mg and three P at 2.862, 2.184, 2.185, and 2.252 Å, respectively, with bond angles 96.2°, 102.7°, 109.9°, 111.3°, 111.5°, and 124.2° [27]. Each Mg is coordinated to six P. A projection of the structure on the (010) plane of the unit cell is depicted in Figure 6; MgP_4 is a Zintl phase containing infinite polyanionic chains of catenated phosphorus. The solid state ^{31}P NMR spectra of MgP_4 are given in Figure 7. Two asymmetric ^{31}P resonances of comparable intensity are observed in the static spectrum, as expected from equal numbers of phosphorus in the two coordination sites. The spinning spectrum resolves the two isotropic chemical shifts A and B at -109.2 and -6.1 ppm, respectively. The upfield resonance A arising from the P atom with greater shielding is assigned to P_1 which is bonded to two metallic atoms, in contrast to P_2 which is bonded to only one metal. Since there is considerable P-P bonding in MgP_4, significant P-P homonuclear dipole-dipole broadening might be expected. However, the isotropic signals at A and B are relatively narrow, indicating that MAS at moderate spinning speeds is very effective in reducing this broadening effect. For example, the expected dipole-dipole broadening of two protons separated by 2 Å is approximately 10 kHz [1]. This is reduced by a factor of six for two ^{31}P

nuclei at the same separation because of the relative magnetogyric ratios of ^{1}H and ^{31}P [1].

$CdPS_3$. $CdPS_3$ is considered to be a layered thiophosphate containing $(P_2S_6)^{4-}$ clusters [28,29]. The structure can be derived from that of cubic, two-dimensional $CdCl_2$: one can consider a close-packed sulfur array with all octahedral sites filled in every other layer. In $CdCl_2$, Cd fills these octahedral sites but in $CdPS_3$ they are half-filled by Cd and half by P-P units, and distortions lower the symmetry to monoclinic (C2/m; a = 6.218(1), b = 10.763(2), c = 6.867(1) Å, β = 107.58(1)°; Z = 4 formula weights per unit cell) [30]. All phosphorus atoms are crystallographically equivalent and occupy the Wyckoff 4i position. The sulfur atoms are of two types, one-third occupying another set of 4i sites, with the remainder in the 8j general positions. Cadmium atoms occupy the 4g sites. The local geometry about phosphorus is shown in Figure 8 [29]. Each P is 4-coordinate to three S and one P, with bond lengths of 2.032(2) and 2 @ 2.027(1) Å to sulfur, and 2.222(2) Å to phosphorus [30]. The local geometry about P is therefore pseudo-tetrahedral, and its chemical behavior indicates a positive formal valence, in contrast to that in ZrP, Mg_3P_2, and MgP_4. The ^{31}P solid state NMR spectra are shown in Figure 9. The MAS spectrum reveals a single isotropic resonance A as expected since all phosphorus atoms are crystallographically equivalent. As in MgP_4, the narrowness of the isotropic signal at +109.4 ppm indicates that MAS has effectively removed any P-P homonuclear dipole-dipole broadening which would arise from the P-P bonding in $CdPS_3$.

CONCLUSIONS

The ^{31}P MAS NMR spectra of ZrP, Mg_3P_2, MgP_4, and $CdPS_3$ indicate that crystallographically different phosphorus atoms can be distinguished. Different degrees of chemical anisotropy about phosphorus are reflected in the broad, asymmetric shapes of the static spectra. The isotropic chemical shifts revealed in the MAS spectra were assigned to crystallographically different phosphorus sites by considering the structural details of each compound.

ACKNOWLEDGMENTS

The authors thank Roxanne Quintana for assistance in obtaining the NMR spectra, David Decker for carrying out the synthesis of $ZrP_{0.92}$, and Dr. Charlotte Lowe-Ma for helpful structural discussions and computation of the bond angles in Mg_3P_2. The comments of Professor Gregory Geoffroy of Pennsylvania State University are much appreciated. This work was supported by the Office of Naval Research and the Naval Air Systems Command.

REFERENCES

1. Fyfe, Colin A., *Solid State NMR for Chemists*; C.F.C. Press: Ontario, (1983).
2. Fukushima, E. and Roeder, S. B. W., *Experimental Pulse NMR*; Addison-Wesley: Reading, Mass., (1981).
3. O'Donnell, D. J., Bartuska, V. J., Palmer, A. R. and Sindorf, D. W., *Amer. Lab.* **18**:96 (1986).
4. Turner, G. L., Kirkpatrick, R. J., Risbud, S. H. and Oldfield, E., *Am. Ceram. Soc. Bull.* **66**, 656-663 1987).
5. Thomas, J. M., Fyfe, C. A., Ramdas, S., Klinowski, J. and Gobbl, G. C., *J. Phys. Chem.* **86**, 3061, (1982) and references cited therein.
6. Klinowski, J., Thomas, J. M., Fyfe, C. A. and Hartman, J. S., *J. Phys. Chem.* **85**, 2590, (1981) and references cited therein.
7. Mavel, G., In *Annual Reports on NMR Spectroscopy*, Vol. **5B**; Mooney, E. F., Ed.; Academic Press: New York, (1973).
8. Carty, A. J., Maclaughlin, S. A. and Taylor, N. J., *J. Organometallic Chem.* **204**, C27-C32, (1981).
9. Petersen, J. L. and Stewart, Jr., R. P., *Inorg. Chem.* (1980), **19**, 186, (1981).
10. Garrou, P. E., *Chem. Rev.* **81**, 229, (1981).
11. Jakeman, R. J. B., Cheetham, A. K., Clayden, N. J. and Dobson, C. M., *J. Am. Chem. Soc.* **107**, 6249, (1985).
12. Mudrakovskii, I. L., Shmachkova, V. P., Kotsarenko, N. S. and Mastikhin, V. M., *J. Phys. Chem. Solids*, **47**, 335. (1986).
13. Villa, M., Carduner, K. R. and Chiodelli, G., *J. Solid State Chem.* **69**, 19, (1987).
14. Duncan, T. M., Karlicek, Jr., R. F., Bonner, W. A. and Thiel, F. A. *J. Phys. Chem. Solids* **45**, 389, (1984).

15. Ryan, M. A., Peterson, M. W., Williamson, D. L., Frey, J. S., Maciel, G. E. and Parkinson, B. A., *J. Mater. Res.* **2**, 528, (1987).

16. Vanderah, T. A. and Nissan, R. A. submitted for publication.

17. Schoenberg, N., *Acta Chem. Scand.* **8**, 226, (1954).

18. Irani K. S. and Gingerich, K. A., *J. Phys. Chem. Solids*, **24**, 1153, (1963).

19. Hewston, T. A., *Solid State Chem.* **69**, 179, (1987).

20. Covino, J., Dragovich, P., Lowe-Ma, C. K., Kubin, R. F. and Schwartz, R. W. *Mater. Res. Bull.* **20**, 1099, (1985),.

21. Wyckoff, R. W. G., *Crystal Structures*, 2nd ed.; Interscience: New York; Vol. 1, pp. 146-148, (1963).

22. Stackelberg, M. V. and Paulus, R., *Z. Phys. Chem.* **22B**, 305, (1933).

23. Ref. 21, Volume 2, pp. 2-6.

24. Wells, A. F., *Structural Inorganic Chemistry*, 4th ed.; Clarendon: Oxford, p. 451, (1933).

25. Kessemeier, H. and Norberg, R. E., *Phys. Rev.* **155**, 321, (1967).

26. Gibby, M. G., Pines, A., Rhim, W. K. and Waugh, J. S., *J. Chem. Phys.* **56**, 991 (1972).

27. von Schnering, H. G. and Menge, G. Z., *Anorg. Allg. Chem.* **422**, 219, (1976).

28. Ohno, Y. and Hirama, K., *J. Solid State Chem.* **63**, 258, (1986).

29. Mercier, H., Mathey, Y. and Canadell, E., *Inorg. Chem.* **26**, 963, (1987).

30. Ouvrard, G., Brec, R. and Rouxel, J., *Mater. Res. Bull.* **20**, 1181, (1985).

TABLE 1

Compound	Signal[a]	δ, ppm[b]	Site[c]	Comments
ZrP	A	+128.4	2d	two isotropic chemical shifts; large CSA[d]
	B	+187.5	2a	
Mg_3P_2	A	-262.3	24d	two isotropic shifts in a ratio of 3:1
	B	-239.6	8a	
MgP_4	A	-109.2	4e	two isotropic shifts; large CSA
	B	-6.1	4e	
$CdPS_3$	A	+104.9	4i	one isotropic shift; large CSA

[a]See spectra.

[b]Chemical shift relative to 85% H_3PO_4.

[c]Wyckoff crystallographic notation for phosphorus position(s); see text and figures.

[d]Chemical shift anisotropy.

FIGURE CAPTIONS

Figure 1 Coordination geometries of phosphorus in ZrP; octahedral: 2a site, trigonal prismatic: 2d site.

Figure 2 Solid state ^{31}P NMR spectra of hexagonal ZrP.

(a) Static spectrum; inset depicts the shapes of the two axially symmetric resonances.

(b) MAS spectrum; the isotropic signals A and B are flanked by first- to fourth-order spinning sidebands a_1 to a_4 and b_1 to b_4, respectively.

Figure 3 Solid state ^{31}P NMR spectra of $ZrP_{0.92}$ which is a mixture of cubic and hexagonal forms of ZrP.

(a) Static spectrum.

(b) MAS spectrum; isotropic signals A and B are flanked by spinning sidebands a_1 to a_3 and b_1 to b_3, respectively; signal A is assigned to trigonal prismatic phosphorus (2d site) and B to octahedral phosphorus (2a site).

Figure 4 Coordination geometries of phosphorus in anti-bixbyite-type Mg_3P_2; both the 24d and the 8a sites are 6-coordinate and are derived from cubic 8-coordination by removing two vertices.

Figure 5 Solid state ^{31}P NMR spectra of Mg_3P_2.

(a) Static spectrum.

(b) MAS spectrum; isotropic signals A and B are flanked by first-order spinning sidebands a_1 and b_1; relative intensities assign A to 24d site and B to 8a site.

Figure 6 Projection of the MgP_4 structure on the (010) plane of the unit cell [25]; P_1 is bonded to two Mg and two P, P_2 to three P and one Mg.

Figure 7 Solid state ^{31}P NMR spectra of MgP_4.

(a) Static spectrum.

(b) MAS spectrum; isotropic signals A and B are flanked by spinning sidebands a_1 to a_3 and b_1 to b_3, sideband b_1 overlaps with a_2 and b_2 with a_1; signal A is assigned to P_1 and B to P_2.

Figure 8 Coordination geometry about phosphorus in $CdPS_3$; P atoms are part of $(P_2S_6)^{4-}$ clusters; all are crystallographically equivalent and 4-coordinate to three S and one P.

Figure 9 Solid state ^{31}P NMR spectra of $CdPS_3$.

(a) Static spectrum.

(b) MAS spectrum; one isotropic signal is observed with first- and second-order spinning sidebands; the shoulder observed is due to chemical shift anisotropy or an impurity not detectable by X-ray diffraction.

TABLE CAPTION

TABLE I. ^{31}P MAS NMR Summary.

Fig 1

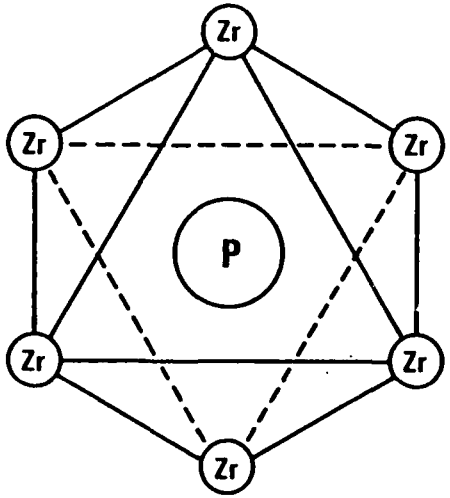

Octahedral

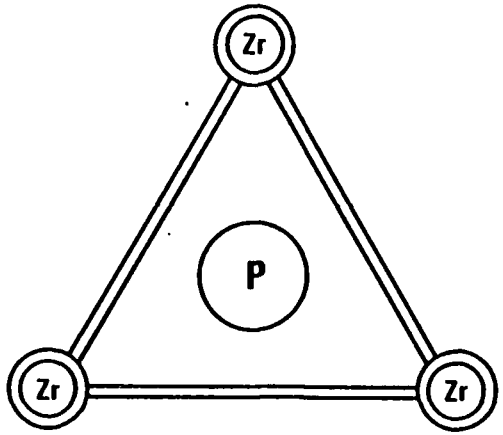

Trigonal Prismatic

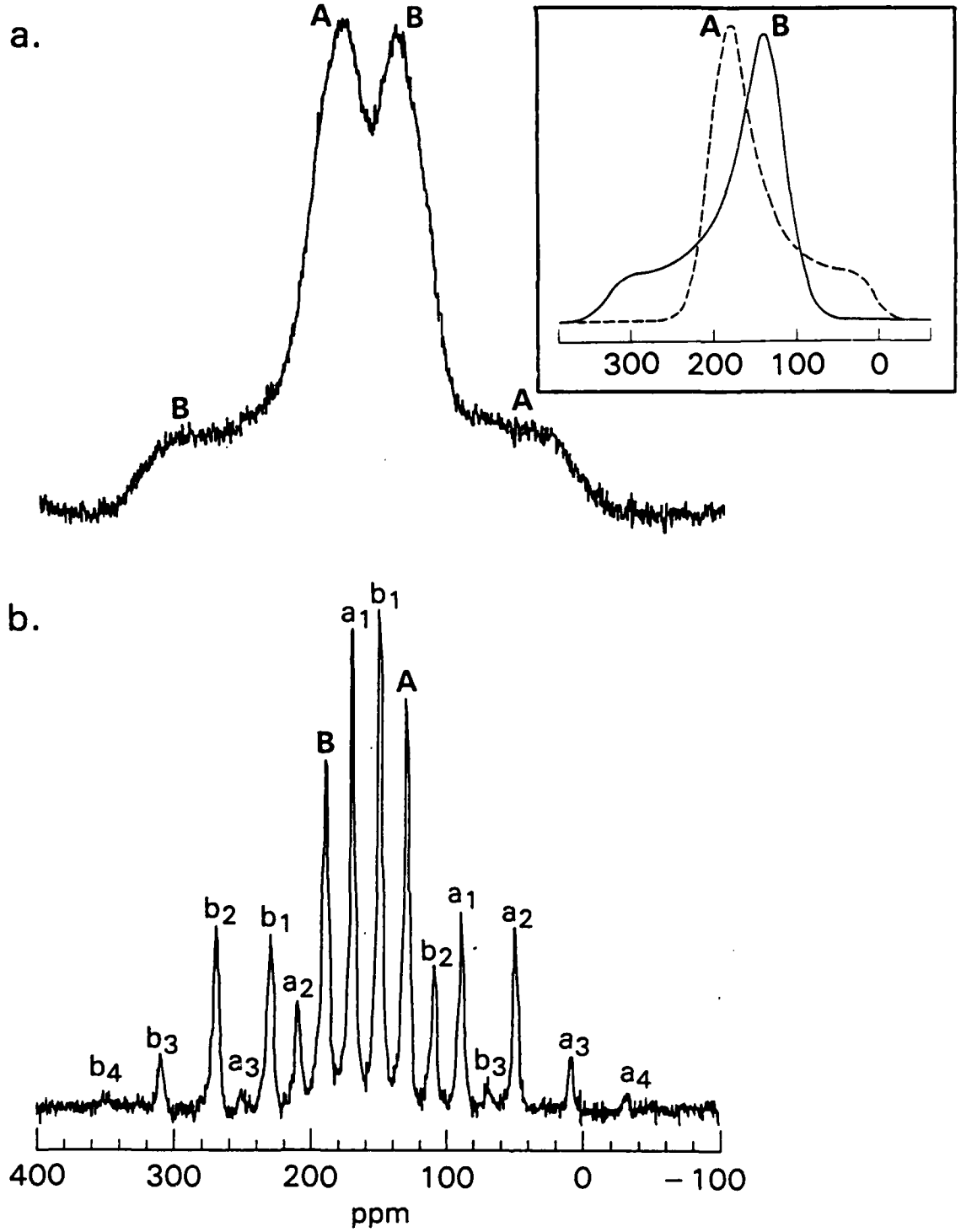
a.
A
B
B
A
A
B
300 200 100 0
b.
a1
b1
A
B
b2
b1
a2
a1
b2
a2
b4
b3
a3
b3
a3
a4
400 300 200 100 0 −100
ppm

Fig 2

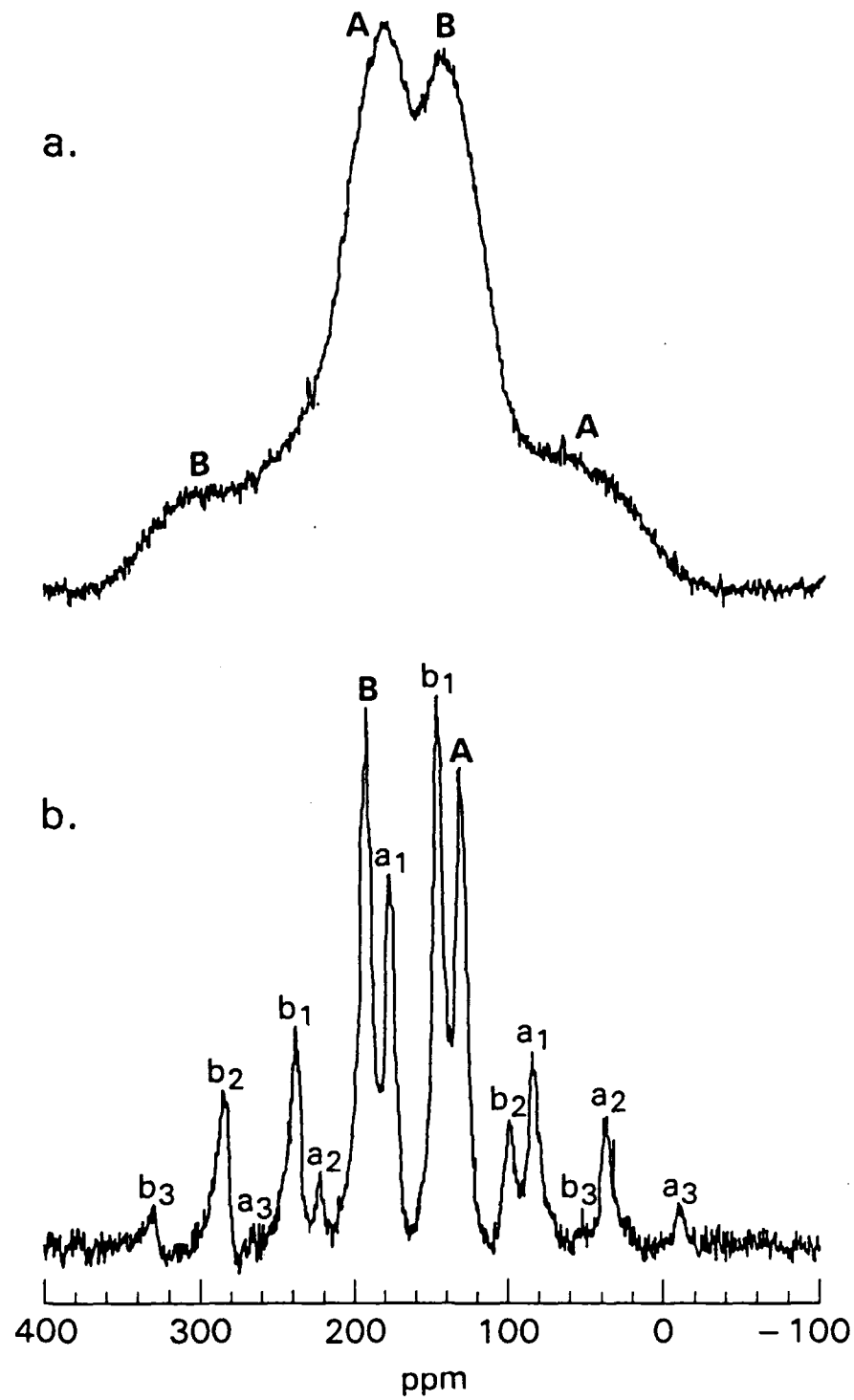
a.
A
B
B
A
b.
B
b1
A
a1
b1
b2
a1
b2
a2
a2
b3
a3
b3
a3
400
300
200
100
0
−100
ppm

Fig 3

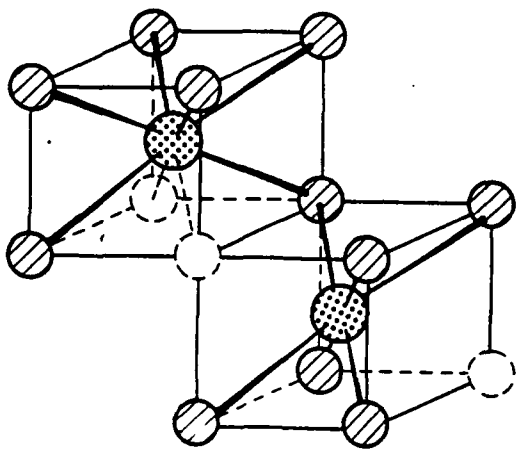

= Mg

= P

Fig 4

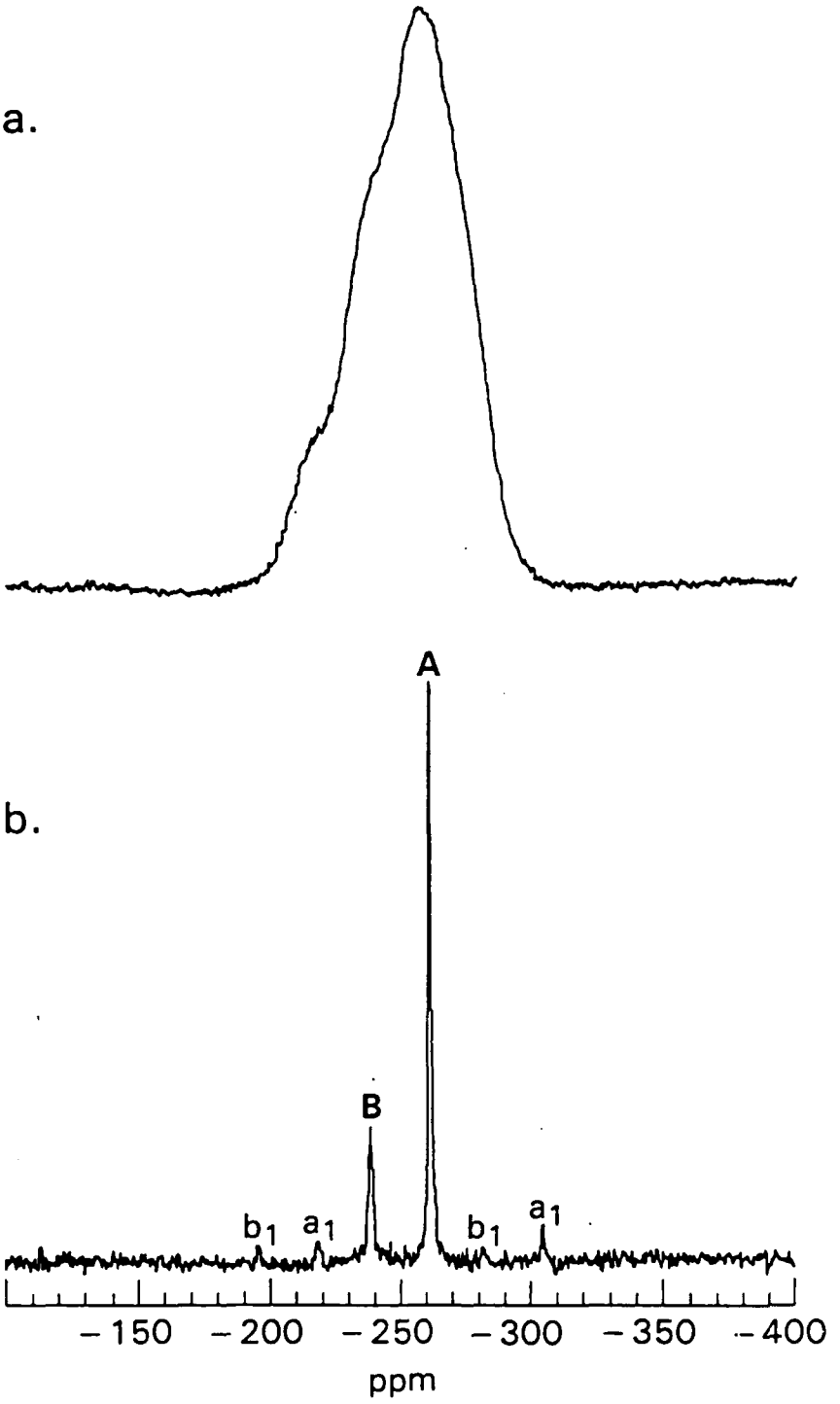

Fig 5

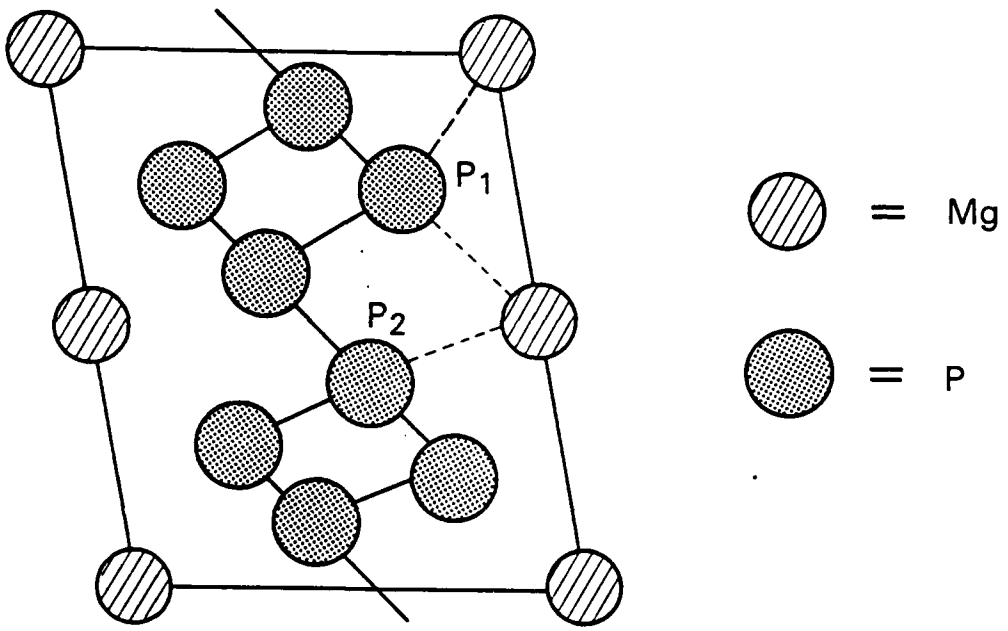

Fig 6

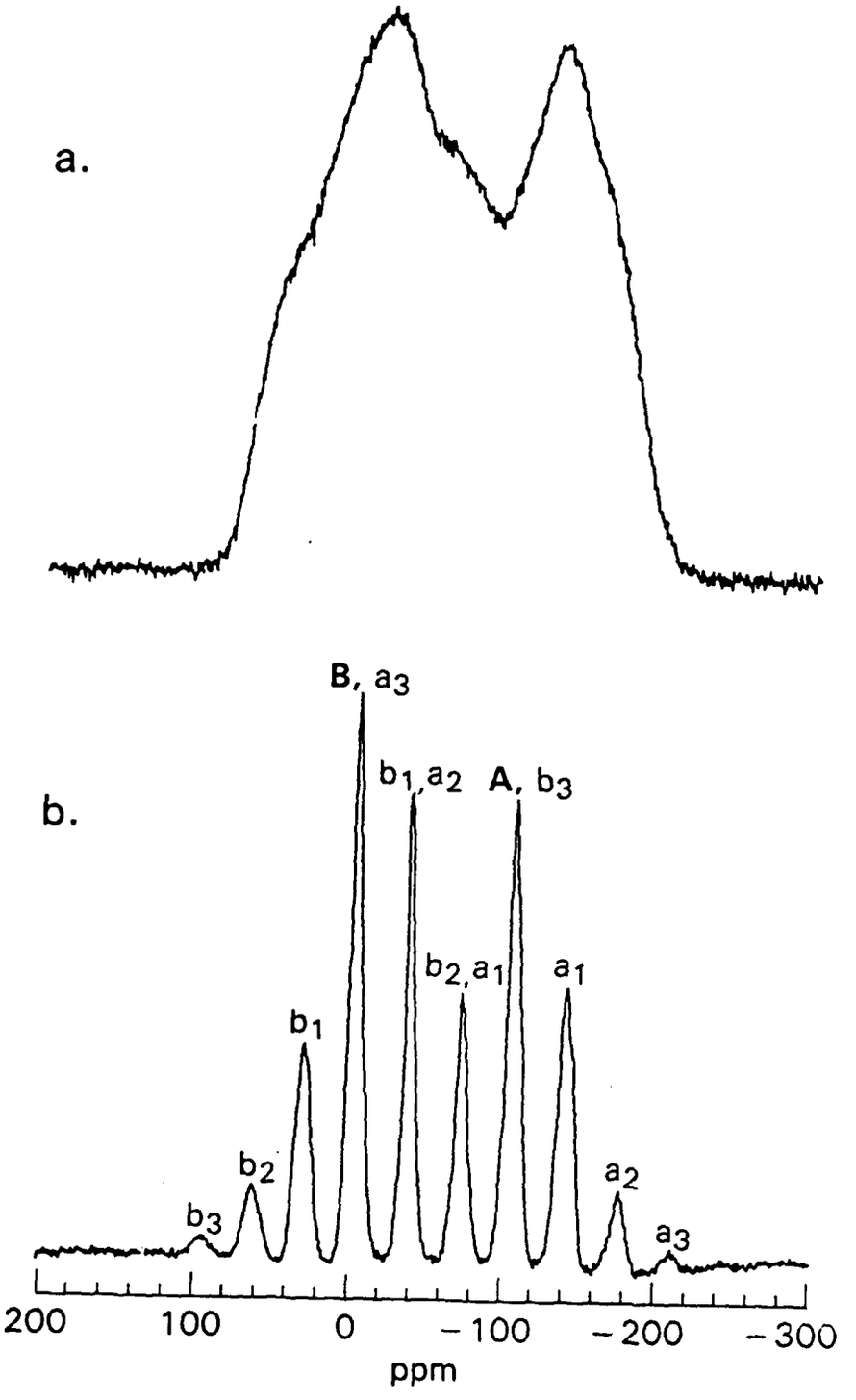

Fig 7

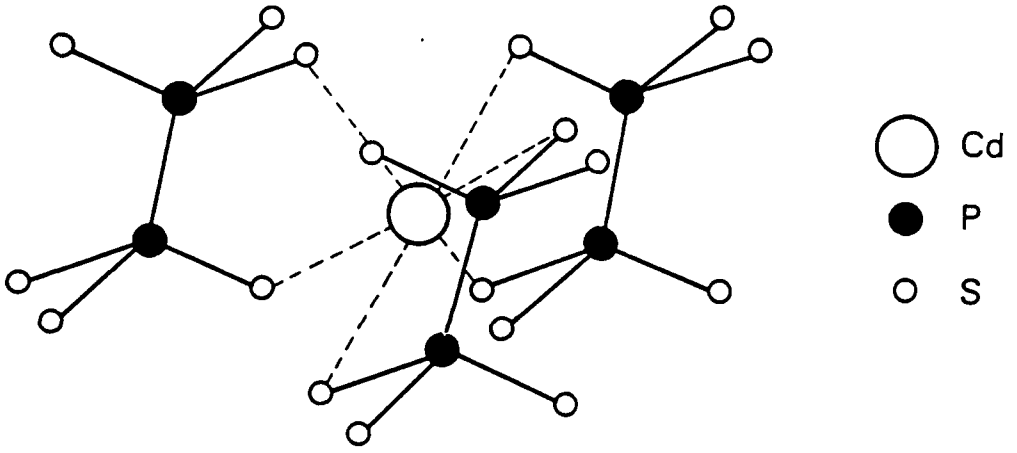

F. 6

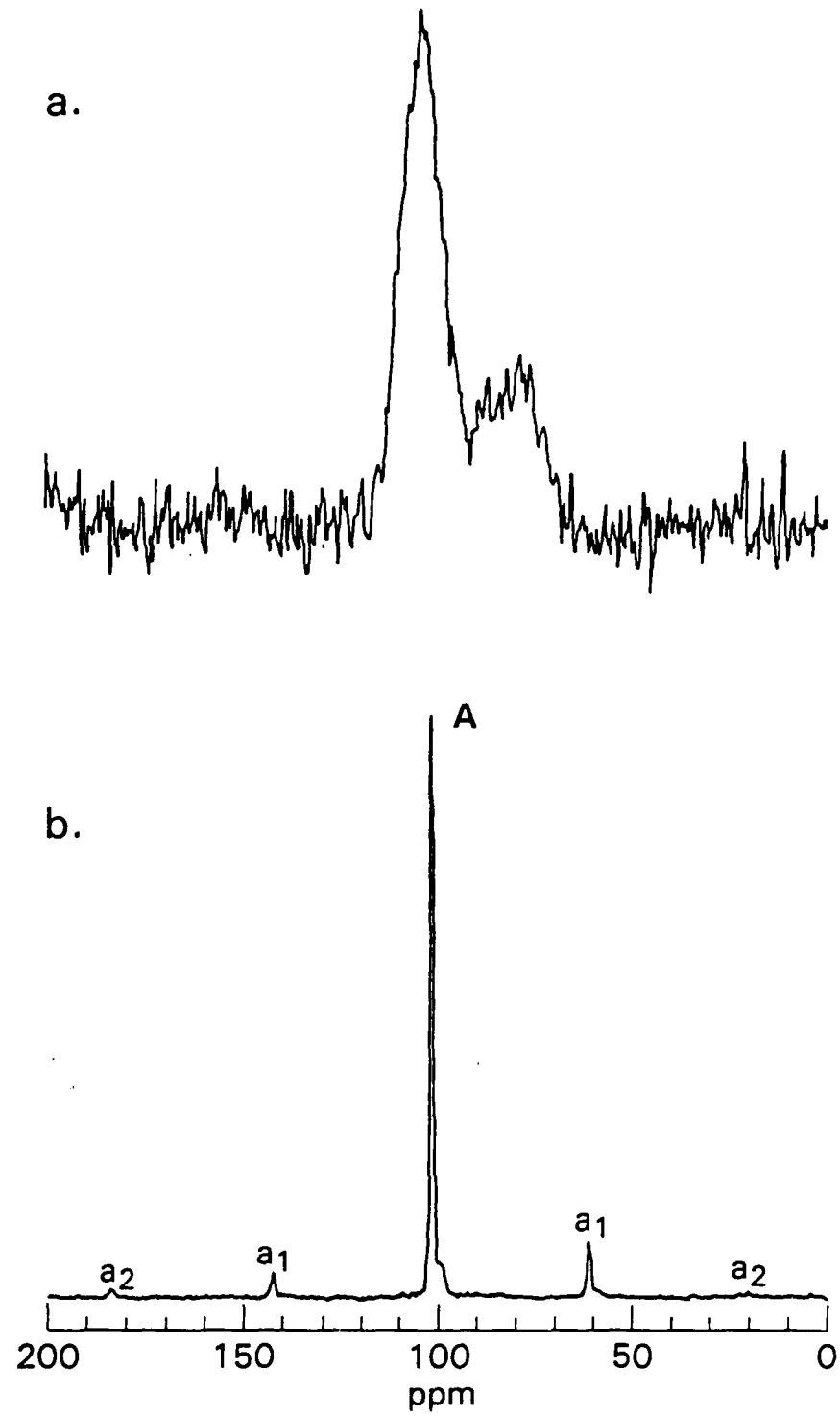

Fig 9

MS 476
J. Phys. Chem. Solids Vol. 00, No. 00, pp. 000–000, 1988
Printed in Great Britain.

0022-3697/88 $3.00 + 0.00

^{31}P MAS NMR OF A II–IV–V_2 CHALCOPYRITE-TYPE SERIES

T. A. VANDERAH and R. A. NISSAN
Chemistry Division, Research Department, Naval Weapons Center, China Lake, CA 93555, U.S.A.

(*Received* 20 *January* 1988; *accepted* 11 *May* 1988)

Abstract—The ^{31}P MAS NMR spectra of the chalcopyrite-type series $ZnSiP_2$, $ZnGeP_2$, and $ZnSnP_2$ are presented. The chemical shifts of −146.7, −58.6, and −92.0 ppm, respectively, are inconsistent with chemical periodicity and structural trends. However, the shifts are consistent with electronegativity considerations and the assignment of Ge as the most electronegative of the three group IV elements. The ^{31}P chemical shifts observed for zinc blende-type GaP and InP are nearly identical at −143.4 and −144.9 ppm, respectively, and are also consistent with electronegativity differences which indicate similar degrees of bond ionicity.

Keywords: Phosphorus-31 MAS NMR, chalcopyrite, $ZnSiP_2$, $ZnGeP_2$, $ZnSnP_2$, InP, GaP.

INTRODUCTION

^{31}P NMR spectra of solid state samples are now relatively easily obtained using the magic angle spinning (MAS) or cross polarization (CP) MAS method [1]. We have obtained the ^{31}P MAS NMR spectra of numerous non-molecular phosphides and find that chemical bond type, local geometry, oxidation state, and, possibly most importantly, the dramatic variability of the hybridization state of phosphorus, combine to make the interpretation of ^{31}P NMR chemical shifts a formidable task [2–4]. Our initial approach was to narrow our attention to three strictly isostructural chalcopyrite-type ternary phosphides—$ZnSiP_2$, $ZnGeP_2$, and $ZnSnP_2$—and explain why the ^{31}P MAS NMR chemical shifts do not correlate with chemical periodicity. This reasoning is extended to interpret the chemical shifts of the related compounds InP and GaP.

EXPERIMENTAL METHODS

$ZnSiP_2$ crystals were grown using the tin flux method which is described in the review of Shay and Wernick [5]. $ZnSiP_2$ needles as long as a centimeter were obtained from a 5 mol.% tin solution of the elements that was heated in a carbon crucible enclosed in an evacuated silica ampule to 1110°C at 125° day^{-1} held at maximum temperature for 12 h, then cooled at 5° h^{-1} to 310°C followed by room-temperature quenching. The orange crystals were recovered from hot concentrated HCl. In one experiment, brilliant black polyhedral crystals of $ZnSnP_2$ were simultaneously obtained. $ZnSiP_2$ powder was prepared by reacting stoichiometric quantities of the elements in a carbon crucible enclosed in an evacuated silica ampule at 1050°C for 7 days. $ZnGeP_2$ powder and crystals were obtained from A. Wold of Brown University. InP and GaP were obtained commercially (Alfa; 99.99 and 99.9%, respectively).

Products were identified by X-ray diffraction using Cu Kα radiation. Powders were characterized using a Scintag PAD V diffractometer; powder diffraction patterns for crystals were obtained using the Gandolfi camera method. All diffraction data were attributable to the expected phases, and unit cell parameters obtained from least-squares refinements were in good agreement with literature values [5].

^{31}P NMR spectra were obtained with an NT-200 WB spectrometer equipped with a MAS probe. The probe was tuned to 81 MHz and an external sample of 85% phosphoric acid was used as the reference standard. Samples were ground and packed into a 7 mm diameter rotor and spun at 3–5 kHz. Occasionally, non spinning spectra were recorded. When sample quantities were limited, 5 mg of crystalline material was found to be sufficient. These samples were ground and mixed with KBr prior to loading. Spectra were acquired by a one-pulse method using a 30° pulse and a 10 s recycle time. Measurements of T_1 were made on $ZnSiP_2$ using the progressive saturation method, and were estimated to be 9 s at a spinning speed of 3.5 kHz. The variation of T_1 with spinning speed and applied field was not investigated. In nearly all cases, spectra were obtained in an hour or less.

RESULTS AND DISCUSSION

$ZnSiP_2$, $ZnGeP_2$, and $ZnSnP_2$ adopt the chalcopyrite ($CuFeS_2$) structure (space group $I\bar{4}2d$, $Z = 4$), which is illustrated in Fig. 1. The structure is a tetragonal superlattice of the cubic zinc blende structure with a c/a ratio approximately equal to 2.† All phosphorus atoms are crystallographically equivalent, as are all group II and group IV atoms. As seen

† $ZnSnP_2$ converts to the zinc blende form above 720°C [5, 6] as cation disorder sets in.

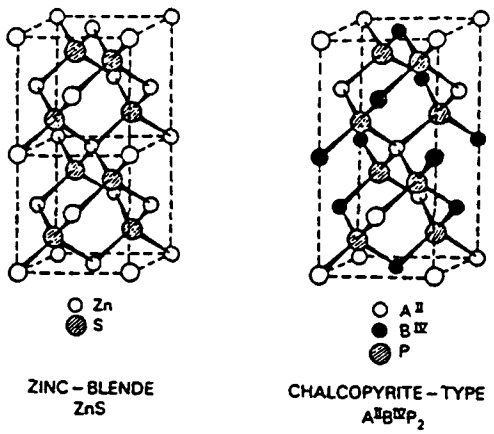

Fig. 1. Cubic zinc blende and the related tetragonal chalcopyrite structures. In the chalcopyrite-type $A^{II}B^{IV}P_2$, each A and B is bonded to four P, and each P is bonded to two A and two B.

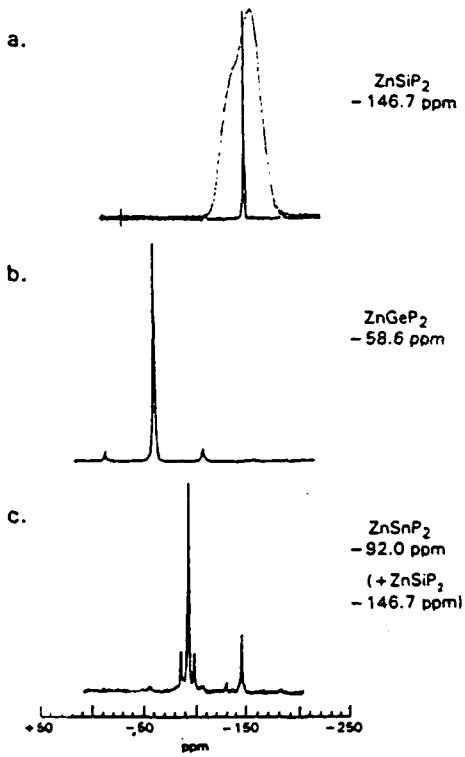

Fig. 2. ^{31}P MAS NMR spectra of the chalcopyrite-type series $ZnSiP_2$, $ZnGeP_2$, and $ZnSnP_2$. The broad, non-spinning spectrum of $ZnSiP_2$ is superimposed on the MAS spectrum in (a): $\sigma_\perp \approx -150$, $\sigma_\parallel \approx -118$ ppm. In (c), the average one-bond J-coupling for $^{119,117}Sn$ to ^{31}P is 1132.9 Hz.

in Fig. 1, the II and IV atoms are all bonded to four phosphorus atoms, while each phosphorus is coordinated to two II and two IV atoms. A key structural feature is that the $B^{IV}P_4$ tetrahedra tend to be regular, causing the other tetrahedra to distort slightly. This is termed the tetragonal distortion and is quantified by the deviation of the c/a ratio from 2. The crystallographic x-parameter locates the phosphorus atoms and depends on the difference between the chemical bonding of phosphorus to the II and IV atoms. In the structure of cubic zinc blende, the x-parameter is 0.25. In II–IV–V_2 compounds, the tendency is that $x > 0.25$ and $c/a < 2$, indicating that the bonds between phosphorus and the IV atoms are shorter than those to the II atoms. The structural parameters for $ZnSiP_2$, $ZnGeP_2$, and $ZnSnP_2$ are listed in Table 1.

For each structural parameter, the changes that occur in going from $ZnSiP_2$ to $ZnGeP_2$ are smooth and consistent with chemical periodicity. The largest disparity in Zn—P and IV—P bond lengths occurs in $ZnSiP_2$ and the tetrahedra about P are the most distorted, with three angles less than the three greater than 109.5°. This distortion and the disparity in bond lengths decreases in $ZnGeP_2$ and is non-existent in the tin analog. All the tetrahedra in $ZnSnP_2$ are regular with identical Zn—P and Sn—P bond lengths: its facile conversion to the statistically disordered zinc blende form is therefore predictable.

The ^{31}P MAS NMR spectra for the three chalcopyrite-type phosphides are shown in Fig. 2. spectral parameters are collected in Table 2. In Fig. 2(a) the broad, non-spinning spectrum of $ZnSiP_2$ is superimposed on the MAS spectrum. The asymmetric shape of the static resonance reflects the chemical anisotropy about phosphorus due to its 4-coordination to two Zn and two Si. The spinning speed is sufficient to reduce the phosphorus chemical shift anisotropy so that isotropic signals are observed in the MAS spectra of all three compounds. The

Table 1. Structural parameters for chalcopyrite-type $ZnSiP_2$, $ZnGeP_2$, and $ZnSnP_2$ ($I\bar{4}2d$, $Z = 4$)†

Compound	Color	a(Å)	c(Å)	Vol mol^{-1} (Å^3)	c/a	x	Bond lengths (Å) Zn—P	Bond lengths (Å) IV—P	Bond angles around P (degrees)
$ZnSiP_2$	Orange	5.40	10.44	76.1	1.93	0.2691	2.37	2.25	2@108.4, 2@111.2, 104.5, 112.8
$ZnGeP_2$	Red	5.46	10.72	79.9	1.96	0.2582	2.38	2.33	2@109.1, 2@110.2, 107.3, 110.9
$ZnSnP_2$	Black	5.65	11.30	90.2	2.00	0.2500	2.45	2.45	6@109.5

† Crystallographic data are from Ref. 5; bond lengths and angles were calculated from these data at NWC.

Table 2. ^{31}P MAS NMR spectral parameters

Compound	Chemical shift (ppm)†	Line width (Hz)‡
$ZnSiP_2$	−146.7	146
$ZnGeP_2$	−58.6	141
$ZnSnP_2$	−92.0	112
GaP	−143.4	320
InP	−144.9	4040

† Referenced to external H_3PO_4 (85%).
‡ Line width measured at half-height.

satellite peaks in the spectra of $ZnSiP_2$ and $ZnGeP_2$ are spinning sidebands; the spectrum of $ZnSiP_2$ impurity is seen in that of $ZnSnP_2$. The two satellites closest to the largest, isotropic peak in the spectrum of $ZnSnP_2$ arise from scalar coupling to ^{117}Sn and ^{119}Sn [6]; the remaining satellites are first-order spinning sidebands. In contrast to the trends in structural parameters, which parallel chemical periodicity, the chemical shift of $ZnSnP_2$ lies between that of the silicon and germanium analogs.

The chemical shifts correlate well, however, with relative electronegativities and predicted bond ionicities. Considerable controversy exists over the assignment of electronegativity values to Si, Ge, and Sn [7]. Certain chemical evidence indicates that Ge is more electronegative than Si or Sn; unusual chemical behavior of germanium may be related to its periodic occurrence just after the first filling of the *d*-orbitals. Electronegativity values from three different scales and the covalent radii for Si, Ge, Sn, and P [8] are listed in Table 3. The electronegativity difference, $\Delta\chi$, between phosphorus and the group IV element is also tabulated. For Si, Ge, and Sn, the three electronegativity scales assign the highest value to Ge. The resulting electronegativity difference between phosphorus and the group IV element is lowest for the Ge—P bond and highest for the Si—P bonding interaction. this indicates that the Si—P bond has the largest degree of ionic character while the Ge—P bond is the least ionic. Therefore, the shift of electron density from the group IV element onto phosphorus is predicted to be largest in $ZnSiP_2$, less in $ZnSnP_2$, and smallest in $ZnGeP_2$. This is consistent with the observed chemical shifts in the ^{31}P NMR spectra of the three compounds: the ^{31}P resonance in $ZnSiP_2$ is the farthest upfield, indicating the highest degree of shielding. The chemical shift for $ZnGeP_2$ is the farthest downfield, indicating the least shielding, and the $ZnSnP_2$ chemical shift value is intermediate.

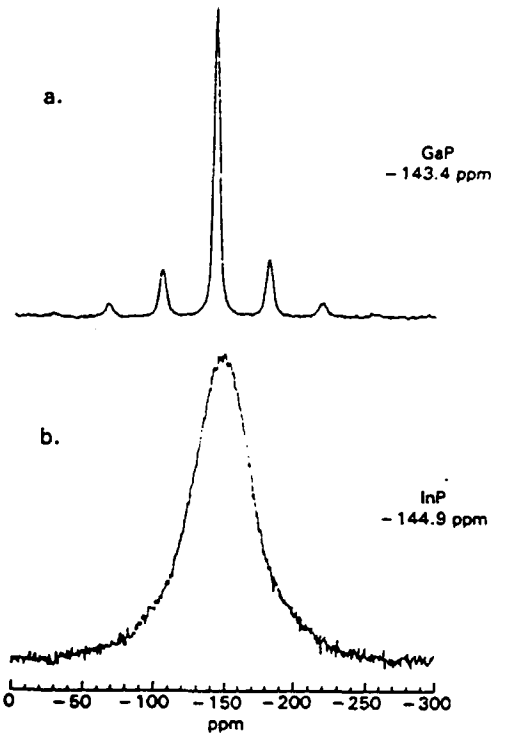

Fig. 3. ^{31}P MAS NMR spectra of zinc blende-type GaP and InP.

The Allred–Rochow electronegativity values for P, Si, Ge, and Sn [8] are also consistent with the downfield position of the $ZnGeP_2$ signal; however, on this scale Si and Sn are assigned nearly equal electronegativities.

GaP and InP both adopt the cubic zinc blende structure; their ^{31}P MAS NMR spectra are shown in Fig. 3 and the spectral parameters are given in Table 2. Broadening of the resonance in InP due to quadrupolar coupling with the spin 9/2 ^{115}In nucleus is not completely removed by MAS. The Pauling scale assigns nearly equal electronegativities to Ga and In, 1.81 and 1.78, $\Delta\chi = 0.38$ and 0.41 for the Ga—P and In—P bonds, respectively. This is consistent with the nearly identical ^{31}P chemical shifts given in Table 2, the In—P bond being just slightly more ionic and thus further upfield. The ^{31}P NMR results for GaP and InP are consistent with those reported by Duncan *et al.* [9], who also observed nearly equal chemical shifts for the two compounds, in contrast to an earlier report of a 65 ppm difference between the signals [10].

Table 3. Covalent radii and electronegativity values

Element	r_{cov} (Å)	χ; $\Delta\chi$ Pauling	Sanderson	Mulliken-Jaffé
Si	1.18	1.90; 0.29	1.74; 0.42	2.25; 0.54
Ge	1.22	2.01; 0.18	2.31; −0.15	2.50; 0.29
Sn	1.40	1.96; 0.23	2.02; 0.14	2.44; 0.35
P	1.10	2.19	2.16	2.79

CONCLUSIONS

The chemical shifts in the ^{31}P MAS NMR spectra of the isostructural series $ZnSiP_2$, $ZnGeP_2$, and $ZnSnP_2$ are consistent with the assignment of electronegativity values Ge > Sn > Si. The results are consistent with group IV-phosphorus electronegativity differences calculated from the Pauling, Sanderson, and Mulliken-Jaffé electronegativity scales. Nearly identical ^{31}P chemical shifts observed for GaP and InP are also consistent with relative bond ionicities as indicated by electronegativity differences. Despite the qualitative and elusive nature of the concept of electronegativity, electronegativity scales continue to provide an important tool for the chemical investigator.

Acknowledgements—The authors thank Dr Charlotte Lowe-Ma for computing the bond lengths and angles in Table 1 and Roxanne Quintana for assistance in obtaining the NMR spectra. This work was supported by the Office of Naval Research and the Naval Air Systems Command.

REFERENCES

1. Fyfe C. A., *Solid State NMR for Chemists*, C.F.C. Press, Ontario (1983).
2. Mavel G., in *Annual Reports on NMR Spectroscopy* (Edited by E. F. Mooney), Vol. 5B. Academic Press, New York (1973).
3. Crutchfield M. M., Dungan C. H., Letcher J. H., Mark V. and VanWazer J. R., *Topics in Phosphorus Chemistry* (Edited by M. Grayson and E. J. Griffith), Vol. 5. Interscience, New York (1967).
4. Garrou P. E., *Chem. Rev.* **81**, 229 (1981).
5. Shay J. L. and Wernick J. H., *Ternary Chalcopyrite Semiconductors: Growth, Electronic Properties, and Applications*, Chap. 2. Pergamon Press, New York (1975).
6. Ryan M. A., Peterson Mark W., Williamson. D. L., Frey James S., Maciel Gary E. and Parkinson B. A., *J. Mater. Res.* **2**, 528 (1987).
7. Cotton F. A. and Wilkinson G., *Advanced Inorganic Chemistry*, 4th edn, p. 374 and references therein. John Wiley, New York (1980).
8. Huheey J. E., *Inorganic Chemistry* (Edited by S. I. Unit), Chaps 4 and 5. Harper & Row (1975).
9. Duncan T. M., Karlicek R. F. Jr, Bonner W. A. and Thiel F. A., *J. Phys. Chem. Solids* **45**, 389–391 (1984).
10. Humphries L. J. and Sears R. E. J., *J. Phys. Chem. Solids* **36**, 1149 (1975).

JOURNAL OF SOLID STATE CHEMISTRY 69, 179–181 (1987)

LETTERS TO THE EDITOR

On the Existence of $MgGeP_2$

T. A. HEWSTON

Chemistry Division, Research Department, Naval Weapons Center, China Lake, California 93555

Communicated by J. M. Honig, March 23, 1987

Present attempts to prepare $MgGeP_2$, a scantily characterized phase which was reported in 1961, have led to the growth of crystals for which the X-ray data agree with that reported previously for $MgGeP_2$. The X-ray diffraction experiments and chemical analysis by SEM indicate that the crystals obtained here are pure germanium. Reasons are presented for the possible nonexistence of $MgGeP_2$.

Introduction

Considerable interest has existed in the synthesis and properties of II-IV-V_2 and I-III-VI_2 semiconductors as ternary analogs of the well-known III-V and II-VI binaries (*1*). The structures displayed by the binary compounds are diamond-like with the two elements occupying alternate tetrahedral sites. This structural theme is maintained by the ternary compounds, but cation-ordering usually occurs which results in the anisotropic (tetragonal) chalcopyrite structure. Compared to the binary analogs, the ternary compounds display a wide range of band gap values; in addition, some of them possess nonlinear optical properties. These materials have therefore received considerable attention for electronic and optical applications.

The preparation of $MgGeP_2$ was first reported in 1961 by Folberth and Pfister (*2*); a sphalerite-type cell with statistical cation disorder was reported with $a = 5.652$ Å—neither the preparative method nor a chemical analysis was given. This work is cited by Wyckoff (*3*) and the "Crystal Data Determinative Tables" (*4*). Spring-Thorpe and Pamplin (*5*, *6*) reported the preparation of single crystals of II-IV-V_2 semiconducting compounds using solution growth from molten tin. The authors report the preparation of $MgGeP_2$ as a cubic phase with $a = 5.654$ Å; an optical energy gap of 2.0 eV is tabulated, but no further characterization is given. $MgGeP_2$ is mentioned in three nonexperimental papers (*7–9*), and the work described above is summarized in the text by Shay and Wernick (*1*).

Our interest in $MgGeP_2$ stemmed from its possible physical and chemical properties; although its existence was reported 25 years ago, little or no characterization has been published. It also appeared unusual and interesting that $MgGeP_2$ would adopt a sphalerite-type structure with a random cation distribution. Only $MgGeP_2$ is reported to adopt this cubic structure as the

0022-4596/87 $3.00

room-temperature equilibrium phase, although four of the other chalcopyrite-type ternaries undergo structural phase transitions to the sphalerite structure at elevated temperatures (*1*). Folberth and Pfister (*10*) suggest that sphalerite-type $ZnSnAs_2$ occurs because the polarizabilities of the Zn–As and Sn–As bonds are similar, as would be expected according to periodic proximities. In contrast, in $MgGeP_2$, the Mg–P bond should be significantly more ionic than the Ge–P bond. In $ZnGeP_2$, with zinc and germanium only two atomic numbers apart, cation-ordering occurs and only the chalcopyrite structure is observed. The occurrence of a random distribution of magnesium and germanium in $MgGeP_2$ therefore seems quite unusual. A study was initiated to prepare this phase and determine its properties.

Experimental Methods

The procedure of Spring-Thorpe and Pamplin (*5*) was repeated to the extent that the reported information permitted; since the melting point of $MgGeP_2$ is not known, it was not possible to deliberately heat to "within about 100°C of the normal melting point of the compound," as the authors state in their generic procedure (*5*). Stoichiometric quantities of red phosphorus, germanium, and magnesium were ground together for 30 min in an agate mortar and pestle. The reactant mixture and sufficient tin shot for a 10 mole% solution were placed in a carbon crucible enclosed in a heavy-walled fused silica sample which was then evacuated and sealed at 6×10^{-5} Torr. Heating was carried out in a 3-zone tube-type furnace: the mixture was heated over 3 days to 1100°C, held there for 12 hr, then cooled at 2.5°/hr to 320°C. It was then quickly reheated to 1000°C, held there 24 hr, and cooled to 620°C at 2.5°/hr; the furnace was then turned off and the ampule removed after cooling to room temperature. The gray reaction plug was placed in concentrated HCl and warmed slightly until all the tin had dissolved as indicated by no further effervescence. A silver-gray granular powder and shiny black pyramidal crystals were isolated. The products were characterized by X-ray diffraction (powder: Scintag PAD V diffractometer, CuKα radiation; crystals: Gandolfi method, Cu$K\alpha$ radiation) and a chemical analysis was performed by SEM (Amray Model 1400, Tracor Northern Model TN2000 X-ray Analyzer).

Results and Discussion

The Gandolfi X-ray diffraction data for the crystals were indexed with a face-centered cubic unit cell, yielding $a = 5.659(1)$ Å. This result is in good agreement with the unit cell parameters of 5.652 (*2*) and 5.654 Å (*5*) which have been reported for $MgGeP_2$. Qualitative chemical analysis of the crystals by SEM, however, indicated that they were pure germanium. The unit cell parameter for pure Ge is 5.65763(4) Å (*4*), and the X-ray diffraction pattern, both *d*-spacings and line intensities, of the crystals obtained in the present study is essentially identical to that of elemental germanium (*11*). Chemical analysis by SEM of the granular powder product indicated that it was rich in phosphorus and magnesium; the X-ray diffraction pattern indicated the presence of MgP_4 and Ge.

The crystals prepared in the present study are elemental germanium, not $MgGeP_2$. In fact, all the reported X-ray data for $MgGeP_2$ are also consistent with that of elemental Ge. In light of (1) the paucity of characterization studies on $MgGeP_2$ despite the report of its isolation 25 years ago, (2) the absence of a specific preparative procedure for the compound, (3) the absence of analytical data on any of the phases previously reported to be $MgGeP_2$, (4) the structural–chemical arguments given above that

it would be unusual for $MgGeP_2$ to form in the sphalerite structure, and (5) the lack of success in the present study to prepare the compound under the given conditions, it is our conclusion that the existence of $MgGeP_2$ is doubtful.

Acknowledgment

This work was supported by funds from the Naval Air Systems Command.

Note added in proof. We appreciate the comment of a referee who pointed out that $MgSiP_2$ is reported (*12*) to decompose in HCl, and therefore so might $MgGeP_2$. Even though no other solvent for the tin flux is mentioned in the single reported synthetic procedure for $MgGeP_2$ (*5*), it was decided to check this point experimentally. Crystal growth of $MgGeP_2$ from the elements in tin flux was again attempted, with a heating/cooling regime according to the procedure for $MgSiP_2$ (*12*). No large crystals were observed in the tin ingot. Elemental phosphorus was present which ignited during decanting of excess tin. The granular product contained extremely small, shiny black crystals; it was divided, and a portion was treated as usual with hot HCl while the remainder was leached with hot mercury (*12*) to remove the tin. The product from the HCl-treatment was a mixture of germanium and MgP_4, as obtained previously. The product from the Hg-treatment, according to X-ray diffraction, contained the same phases.

In a ^{31}P MAS NMR study (with R.A. Nissan) of three-dimensional inorganic phosphides (to be published), we have prepared and obtained the ^{31}P NMR spectra of a number of the II-IV-V_2 chalcopyrite-type semiconductors—including $ZnSiP_2$, $ZnGeP_2$, and $ZnSnP_2$—and the related sphalerite-type GaP. As a final check for the presence of $MgGeP_2$, we compared the ^{31}P MAS NMR spectra of the products obtained from the HCl- and the Hg-treatments. The spectra indicated that the phosphorus-containing phases in both samples were the same, and no indication of sphalerite- or chalcopyrite-type $MgGeP_2$ was observed. We believe that these additional results further confirm the nonexistence of $MgGeP_2$, to date.

References

1. J. L. Shay and J. H. Wernick, "Ternary Chalcopyrite Semiconductors: Growth, Electronic Properties, and Applications," Pergamon, Elmsford, NY (1975).
2. O. G. Folberth and H. Pfister, *Acta Crystallogr.* **14,** 325 (1961).
3. R. W. G. Wyckoff, "Crystal Structures," 2nd ed., Vol. 2, pp. 339, 346, Interscience, New York (1964).
4. "Crystal Data Determinative Tables," 3rd ed. (J. D. H. Donnay and H. M. Ondik, Eds.), pp. C-122, C-123, U.S. Dept. of Commerce, National Bureau of Standards, and Joint Committee on Powder Diffraction Standards (1973).
5. A. J. Spring-Thorpe and B. R. Pamplin, *J. Crystal Growth* **3/4,** 313 (1968).
6. "Crystal Growth" (B. R. Pamplin, Ed.), p. 430, Pergamon, Elmsford, NY (1975).
7. N. A. Goryunova *et al.*, Chem. Abstracts **72,** Abstr. No. 71,806q; *Khim. Svyaz. Krist.* (N. N. Sirota, Ed.), pp. 439–446 (1969).
8. K. Huebner and K. Unser, *Phys. Status Solidi B* **50,** K105 (1972).
9. K. Huebner, *Phys. Status Solidi B* **52,** K33 (1972).
10. O. G. Folberth and H. Pfister, *Acta Crystallogr.* **13,** 199 (1960).
11. "Powder Diffraction File," JCPDS; Swarthmore, PA, Card No. 4-0545.
12. A. J. Spring-Thorpe and J. G. Harrison, *Nature (London)* **222,** 977 (1969).